THE JOURNAL OF PHYSICAL CHEMISTRY A

 VOLUME 113, NUMBER 34, AUGUST 27, 2009

# ARTICLES

## MS-CASPT2 Assignment of the UV/Vis Absorption Spectrum of Diazoquinones Undergoing the Photoinduced Wolff Rearrangement

**Quansong Li,[†] Annapaola Migani,[‡] and Lluís Blancafort*[,†]**

*Institut de Química Computacional, Departament de Química, Universitat de Girona, Girona, Spain 17071, Departament de Química Física, Universitat de Barcelona, Barcelona, Spain 08028*

*Received: May 25, 2009; Revised Manuscript Received: July 14, 2009*

The absorption spectra of *o*-diazobenzoquinone (DBQ), *o*-diazonaphthoquinone (DNQ) and *o*-diazonaphthoquinone-5-sulfonic acid (DNQSH) are computed at the MS-CASPT2 level to assign the experimental UV/vis spectra. These compounds undergo the photoinduced Wolff rearrangement, which is applied in the fabrication of photoresists. The lowest energy broadband around 400 nm corresponds to excitation to the lowest $\pi\pi^*$ state and has a vibrational structure mainly due to the activity of a ring bond inversion and a diazo bending mode. The remaining bands of the spectra arise from $\pi\pi^*$ states, while the states involving the oxygen lone pairs and the in-plane $\pi$ orbitals of the diazo group have low oscillator strengths. The lowest $\pi\pi^*$ state has a nonplanar minimum characterized by an out-of-plane bending of the diazo group and a stretching of the C−N bond. While recent experiments point to an ultrafast, concerted reaction, our results suggest that the process may be asynchronous, and the initial phase dominated by nitrogen elimination.

### Introduction

The conversion of α-diazo ketones into ketenes and their products was first reported by Wolff in 1902.[1] Since then the Wolff rearrangement (WR) has been widely studied and used in organic synthesis,[2,3] $\beta$-peptide design,[4] DNA cleavage[5,6] and photoaffinity labeling.[7] The photoinduced WR is also used in the lithographic production of integrated electronic circuits, and diazonaphthoquinone derivatives are the most common photoactive compounds employed for this application.[8]

Although the chemistry of the photoinduced WR is used in many fields and this reaction has been known for more than 70 years, its mechanism is still under debate (Scheme 1). The focus of the discussion is whether the nitrogen extrusion and the rearrangement occur in a concerted or stepwise manner via a carbene intermediate. A recent femtosecond resolved spectroscopic study of diazonaphthoquinone 5-sulfonate[9] reports the formation of the ketene in the sub-picosecond scale. The prompt formation of the ketene species seems to indicate a concerted reaction mechanism. The sub-picosecond formation of the ketene species has also been reported for a non-quinoid analogue, α-biphenyl-α-diazo acetone,[10] pointing to the concerted mechanism also in this system.

The computation of vertical excitation energies is the starting point to understand the mechanism of the WR from excitation to ketene formation. However, to the best of our knowledge no high-level calculations of the spectrum have been published. Therefore, we have calculated the vertical excitation spectra of diazobenzoquinone (DBQ), diazonaphthoquinone (DNQ) and diazonaphthoquinone sulfonic acid (DNQSH) in vacuum and in water using the multistate multiconfigurational second-order perturbation approach (MS-CASPT2). As the sulfonate substituent is important in the applications (e.g., increases the solubility[11]) but does not participate directly in the WR, the 5-sulfonate DNQ derivative is modeled by its protonated form

* Corresponding author. E-mail: lluis.blancafort@udg.edu.
[†] Universitat de Girona.
[‡] Universitat de Barcelona.

10.1021/jp904853c CCC: $40.75 
Published on Web 08/04/2009

**SCHEME 1**

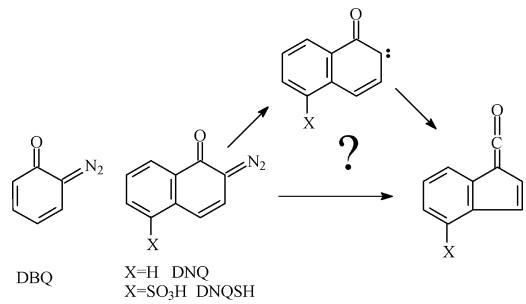


DNQSH. This avoids the complications in the theoretical studies of anionic species.

The absorption spectra of DBQ in water[12] and in argon matrix[13] are very similar and show three bands centered at ~400, ~265, and ~210−220 nm. The UV/vis absorption spectra of DNQ and DNQSH in ethanol glass at 77 K[14] and DNQSH in water[12,15] reveal four different bands. Three bands are nearly the same as those recorded for DBQ and are centered at 400, 260, and 210 nm. The additional band is between 300−330 nm for DNQSH and blue-shifted to 280−310 nm for DNQ. The WR is initiated by using either excitation wavelengths around 400 nm[9] or in the range between 300 and 350 nm.[12,14−16]

Vertical excitation energies of DBQ and DNQ have been previously computed at the semiempirical level neglecting solvent effects. Semiempirical LNDO/S PERTCI calculations assign the three absorption bands of DBQ to $\pi\pi^*$ transitions.[13] The 400 nm band of DNQ was assigned to either a $\sigma\pi^*$ or a $n\pi^*$ transition,[17] or to a $\pi\pi^*$ transition by semiempirical CNDO/S SECI calculations.[18] Our MS-CASPT2 calculations provide a reliable interpretation of the spectrum and attribute the two lowest bands in the spectrum whose wavelengths are used to induce the WR to two different $\pi\pi^*$ states. Moreover the absorption profile of the lowest band in the spectra of DBQ in Ar matrix[13] and DNQ and DNQSH in ethanol glass[14] shows three intense peaks. By means of the computation of the vibrational frequencies and intensities for DNQ we attribute these peaks to the vibrational structure of the lowest energy permitted $\pi\pi^*$electronic transition, and not to contributions from other excited states.

**Computational Details**

The vertical excitation energies of DBQ, DNQ and DNQSH were computed with the MS-CASPT2 method using the 6-311G* basis set. A real level shift parameter of 0.2 and no IPEA[19] modification was used. The ground-state geometries of $C_s$ symmetry optimized at the B3LYP/6-311G* level (Becke-3−Lee−Yang−Parr density functional) are employed in all vertical excitation energy calculations. The complete list of complete active space self-consistent field (CASSCF), complete active space second order perturbation (CASPT2) and MS-CASPT2 vertical excitation energies obtained using two different active spaces (see below) is reported in the Supporting Information (Table SI1). For comparison time-dependent density functional (TD-DFT) vertical excitation energies were also computed with the B3LYP functional and the 6-311G* basis set and are reported in the Supporting Information (Table SI2). The MS-CASPT2 calculations were carried out using MOLCAS version 7.2,[20] while the CASSCF and DFT optimizations and TD-DFT computations were performed with the Gaussian03 program.[21]

The complete active space for DBQ is fourteen electrons in twelve orbitals, which comprises nine $\pi$ orbitals of $a''$ symmetry, and three orbitals of $a'$ symmetry, namely the two in-plane $\pi$ orbitals of the diazo group (labeled $\pi_{NN}$ and $\pi^*_{NN}$), and the oxygen lone pair (labeled $n$). The $\pi$ valence active space (10,9) is used to compute the $\pi\pi^*$ transitions, whereas the (14,12) active space is used for the $\pi\pi^*_{NN}$, $n\pi^*$ and $n\pi^*_{NN}$ transitions involving $a'$ orbitals. For DNQ there are four additional $\pi$ orbitals of $a''$ symmetry giving a total of eighteen electrons in sixteen orbitals, which is computationally not treatable. In this case the $\pi\pi^*_{NN}$, $n\pi^*$ and $n\pi^*_{NN}$ transitions were computed with a (14,12) active space made of 3 $a'$ and 9 $a''$ orbitals, whereas for the $\pi\pi^*$ transitions a (14,12) made of 12 $a''$ orbitals was used. This strategy is specifically designed to provide a balanced and consistent description of $\pi\pi^*$ versus $n\pi^*$ vertical excitations in large chromophores with heteroatoms having several low-lying $n\pi^*$ excited states, and has been successfully applied to assign the absorption spectrum of *o*-nitrobenzaldehyde.[22] The removal of n orbitals permits an increase in the size of the active space used to compute $\pi\pi^*$ vertical excitations and a reduction of the number of roots to be included in the state-averaged wave function. Thus, a six-root state-averaged CASSCF reference wave function with equal weights for all states was used for both sets of vertical excitations. A subset of the active space orbitals that mostly contribute to the description of the vertical excitations for DBQ and DNQ is reported in Figure 1. The CASSCF orbitals for DNQSH are similar to the DNQ ones and are presented in Figure SI1 in the Supporting Information. The vertical excitations of DNQSH were computed using the same active spaces employed for DNQ, as TD-DFT calculations indicate that the orbitals localized on the sulfonic acid residue do not participate in the excitations (Table SI2 and Figure SI2 in the Supporting Information).

Transition dipole moments (TDM) were calculated from the perturbationally modified complete active space configuration interaction (PM-CASCI) wave functions derived from the MS-CASPT2 calculations.[24] These TDM values, combined with the corresponding MS-CASPT2 energies, were used to compute the oscillator strengths according to the relation $f = (2/3)(\mathrm{TDM})^2\Delta E$. The vertical excitations were calculated in the vacuum and in water. The solvent effect is taken into account using the polarizable continuous model (PCM)[25,26] and added in a single-point energy fashion. The nonequilibrium version was used to account for the finite relaxation time of the solvent molecules after the sudden change in electronic distribution caused by the excitation.[27]

The modeling of the vibrational structure of the lowest band in the absorption spectrum of DNQ, which corresponds to the lowest $\pi\pi^*$ excitation ($2^1A'$) is done by assuming that the Franck−Condon (FC) mechanism is the dominant contribution to the vibrational intensity. The vibrational activity is proportional to the parameter $\gamma_i$, which is given by $\gamma_i = 0.5B_i^2$. The $B_i$ parameter is associated with the projection of the difference of the equilibrium geometries of the ground and excited state involved in the electronic excitation, onto the totally symmetric normal modes of the excited state, according to the formula reported in ref 23, $B_i = (\omega_i/\hbar)^{1/2}\cdot(\mathbf{x}_1 - \mathbf{x}_0)\cdot(\mathbf{M})^{1/2}\cdot\mathbf{L}_i$, where $\omega_i$ and $\mathbf{L}_i$ are the $i$th vibrational frequency and mass weighted normal mode of the excited state, $\mathbf{M}$ is the matrix of atomic masses, and $\mathbf{x}_1$ and $\mathbf{x}_0$ are the Cartesian vectors of the excited and ground state optimized geometries. To reduce the computational cost, the DNQ ground and spectroscopic state equilibrium geometries used to compute the vibrational intensities were optimized using a (12,10) active space including 10 orbitals of $a''$ symmetry, and the excited-state frequencies were calculated numerically. In addition to the $C_s$ minimum, another minimum

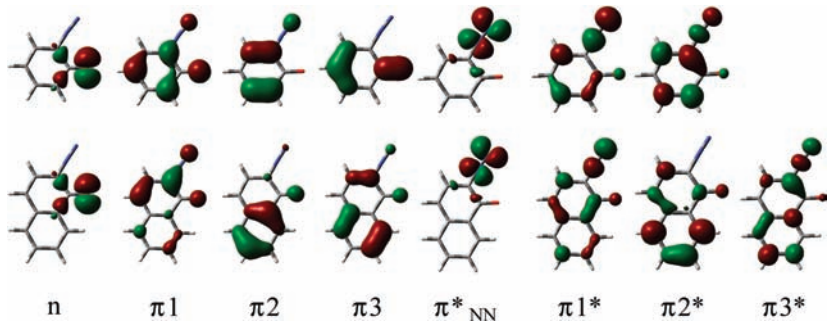


**Figure 1.** DBQ (top) and DNQ (bottom) orbitals involved in the electronic transitions that mostly contribute to the vertical excitations reported in Table 1.

**TABLE 1: MS-CASPT2 Vertical Excitation Energies $\Delta E$ (eV), Excitation Wavelengths $\lambda$ (nm), Oscillator Strengths, $f$, and Most Important Electronic Configurations in Vacuum and in Water Solvent, for DBQ, DNQ, and DNQSH Compared to Experimental Absorption Maxima**

| | | | vacuum | | | water | | | experiment | |
|---|---|---|---|---|---|---|---|---|---|---|
| | state | config | $\Delta E$ (eV) | $\lambda$ (nm) | $f$ | $\Delta E$ (eV) | $\lambda$ (nm) | $f$ | $\Delta E$ (eV) | $\lambda_{max}$ (nm) |
| DBQ | $1^1A''$ | $\pi1 \rightarrow \pi^*_{NN}$ | 2.91 | 427 | 0.000 | 2.95 | 421 | 0.000 | | |
| | $2^1A''$ | $n \rightarrow \pi1^*$ | 3.53 | 352 | 0.000 | 3.84 | 323 | 0.000 | | |
| | $2^1A'$ | $\pi1 \rightarrow \pi1^*$ | 3.24 | 383 | 0.256 | 3.26 | 381 | 0.258 | 3.1 | 400[a,b] |
| | $3^1A'$ | $n \rightarrow \pi^*_{NN}$ | 4.10 | 302 | 0.025 | 4.28 | 290 | 0.005 | | |
| | $4^1A'$ | $\pi2 \rightarrow \pi1^*$ | 4.65 | 267 | 0.150 | 4.55 | 272 | 0.179 | 4.6 | 268[a,b] |
| | $5^1A'$ | $\pi1 \rightarrow \pi2^*$ | 5.22 | 238 | 0.029 | 5.27 | 235 | 0.012 | | |
| | $6^1A'$ | $\pi2 \rightarrow \pi1^*$<br>$\pi3 \rightarrow \pi^*1$ | 5.54 | 224 | 0.052 | 5.59 | 222 | 0.048 | 5.6, 5.8 | 220,[b] 210[c] |
| DNQ | $1^1A''$ | $\pi1 \rightarrow \pi^*_{NN}$ | 3.19 | 389 | 0.000 | 3.23 | 384 | 0.000 | | |
| | $2^1A''$ | $n \rightarrow \pi1^*$ | 4.01 | 310 | 0.000 | 4.26 | 291 | 0.000 | | |
| | $2^1A'$ | $\pi1 \rightarrow \pi1^*$ | 3.16 | 392 | 0.427 | 3.12 | 397 | 0.415 | 3.1 | 400[c] |
| | $3^1A'$ | $\pi1 \rightarrow \pi2^*$<br>$\pi2 \rightarrow \pi1^*$ | 4.23 | 293 | 0.001 | 4.20 | 295 | 0.002 | 4.1 | 300[c] |
| | $4^1A'$ | $\pi3 \rightarrow \pi2^*$ | 4.76 | 260 | 0.112 | 4.64 | 267 | 0.110 | 4.6 | 268[c] |
| | $5^1A'$ | $n \rightarrow \pi^*_{NN}$ | 4.48 | 277 | 0.023 | 4.76 | 260 | 0.004 | | |
| | $6^1A'$ | $\pi1 \rightarrow \pi2^*$<br>$\pi1 \rightarrow \pi3^*$ | 5.01 | 247 | 0.108 | 5.05 | 246 | 0.124 | | |
| | $7^1A'$ | $\pi1 \rightarrow \pi3^*$<br>$\pi2 \rightarrow \pi1^*$ | 5.24 | 237 | 0.291 | 5.16 | 241 | 0.285 | 5.6 | 220[c] |
| DNQSH | $1^1A''$ | $\pi1 \rightarrow \pi^*_{NN}$ | 3.11 | 399 | 0.000 | 3.09 | 401 | 0.000 | | |
| | $2^1A''$ | $n \rightarrow \pi1^*$ | 3.90 | 318 | 0.000 | 4.04 | 307 | 0.000 | | |
| | $2^1A'$ | $\pi1 \rightarrow \pi1^*$ | 2.96 | 418 | 0.401 | 2.94 | 421 | 0.406 | 3.1 | 400[c] |
| | $3^1A'$ | $\pi1 \rightarrow \pi2^*$ | 3.82 | 325 | 0.125 | 3.73 | 333 | 0.093 | 3.9, 3.8 | 315,[c] 325[a] |
| | $4^1A'$ | $n \rightarrow \pi^*_{NN}$ | 4.46 | 278 | 0.035 | 4.28 | 290 | 0.037 | | |
| | $5^1A'$ | $\pi2 \rightarrow \pi2^*$<br>$\pi3 \rightarrow \pi1^*$ | 4.66 | 266 | 0.003 | 4.56 | 272 | 0.095 | 4.6, 4.7 | 268,[c] 262[a] |
| | $6^1A'$ | $\pi1 \rightarrow \pi1^*$[d]<br>$\pi2 \rightarrow \pi1^*$ | 4.76 | 261 | 0.084 | 4.74 | 262 | 0.146 | | |
| | $7^1A'$ | $\pi2 \rightarrow \pi1^*$<br>$\pi1 \rightarrow \pi3^*$ | 5.22 | 238 | 0.267 | 5.09 | 244 | 0.242 | 5.5 | 225[a,c] |

[a] Water from ref 12 for DBQ and ref 12, 15 for DNQ 5-sulfonate derivative. [b] Ar matrix from ref 13. [c] Ethanol glass from ref 14. [d] Two-electron excitation.

of $C_1$ symmetry was optimized on the spectroscopic state. The energies of the optimized structures were recomputed with a (14,12) active space composed of 12 $\pi$ orbitals (Table SI3 in the Supporting Information).

## Results and Discussion

The vertical excitation energies, oscillator strengths and dominant configurations at the MS-CASPT2 level for DBQ, DNQ, and DNQSH in vacuum and in water are presented in Table 1, and the orbitals involved in the electronic transitions that mostly contribute to the description of the vertical excitations are shown in Figure 1. We have calculated two dark states of $^1A''$ symmetry which correspond to electronic promotion from $\pi1$ to the in-plane diazo $\pi^*_{NN}$ orbital and excitation from the oxygen lone pair to the $\pi1^*$ orbital, respectively, and five or six weakly allowed or allowed excited states of $^1A'$ symmetry. One of these states corresponds to the $n\pi^*_{NN}$ transition, and the remaining ones to $\pi\pi^*$ excitations.

Comparison between the vacuum and solution values shows that the solvent effect on the excitation energies is small in most cases. As it may be expected, the $n\pi^*$ and $n\pi^*_{NN}$ states are blue-shifted by at most 0.3 eV in water for all compounds due to the stabilization of the oxygen lone pair. The exception to this trend is the $n\pi^*_{NN}$ excitation of DNQSH, which is red-shifted by 0.2 eV because of the larger dipole moment of the excited state.

The assignment of the experimental bands to the allowed and weakly allowed $\pi\pi^*$ transitions is reported in Table 1. For DBQ, our calculations suggest that the broad band centered at ~400 nm (~3.1 eV) in an argon matrix[13] and in water[12] is due to the $\pi1 \rightarrow \pi1^*$state that is computed at 3.24 eV in vacuum and 3.26 eV in water. The $\pi\pi^*_{NN}$ state is computed at similar energies

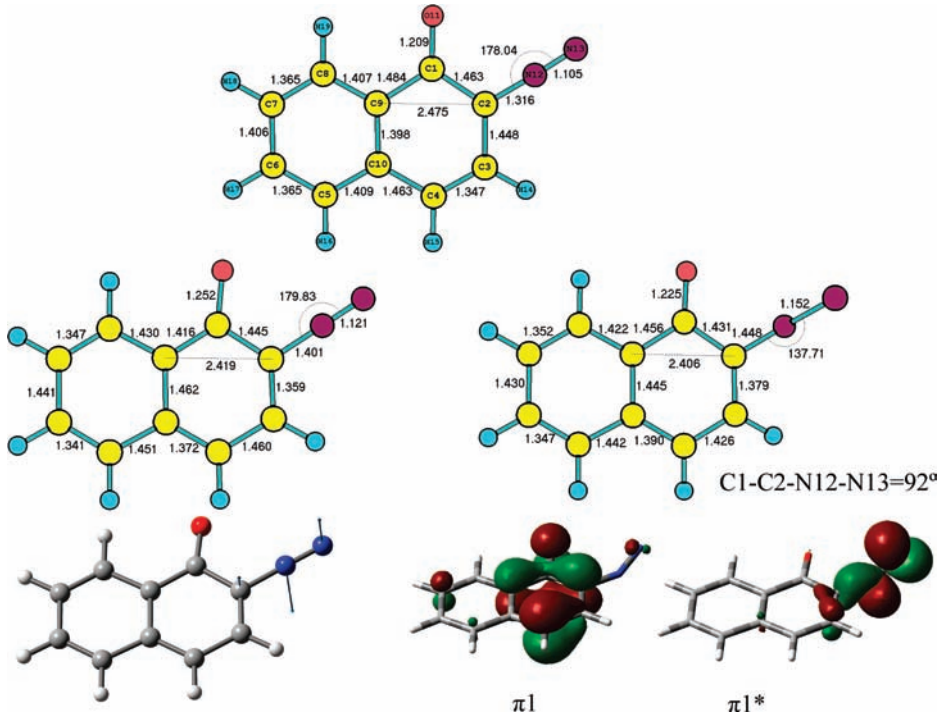


**Figure 2.** (Top) DNQ $S_0$ minimum; (bottom left) $\pi 1 \rightarrow \pi 1^*$ $C_s$ minimum and transition state vector; (bottom right) $\pi 1 \rightarrow \pi 1^*$ $C_1$ minimum and $\pi 1$, $\pi 1^*$ singly occupied molecular orbitals at this geometry. Distances in Å and angles in deg.

(2.91−2.95 eV) but is dark. The second band at ∼268 nm (∼4.6 eV) can be assigned to the $\pi 2 \rightarrow \pi 1^*$ state computed at 4.65 eV in vacuum and 4.55 eV in water. The most intense band at ∼210−220 nm (∼5.6−5.8 eV) should arise from excitation to the $6^1A'$ state predicted at 5.54−5.59 eV with rather high oscillator strength ($f \sim 0.05$).

For DNQ and DNQSH we compare the vertical excitation energies in water with the available absorption spectra in ethanol glass[14] (DNQ and DNQ 5-sulfonate analogue) and in water[12,15] (DNQ 5-sulfonate analogue). Similar to DBQ the lowest energy band at ∼400 nm is attributed to the $\pi 1 \rightarrow \pi 1^*$ state. This state is predicted at 3.12 and 2.94 eV in water in DNQ and DNQSH, respectively, while the dark $\pi\pi^*_{NN}$ state is calculated at 3.23 and 3.09 eV for the two compounds. The shape of the second band observed in the UV/vis spectra in ethanol glass does not allow an accurate determination of the position of maximum absorption, as the absorption profile shows a sequence of three small peaks of similar intensity. This band spans an energy interval of 3.9−4.4 eV in DNQ and 3.8−4.1 eV in the DNQ 5-sulfonate analogue. In DNQ this band could arise from the $3^1A'$ state described by a combination of the $\pi 1 \rightarrow \pi 2^*$ and $\pi 2 \rightarrow \pi 1^*$ configurations, which is reminiscent of the $^1L_b$ state of naphthalene.[28] It is calculated at 4.2 eV, but the calculated oscillator strength is small (0.002). In DNQSH the corresponding transition is dominated by the $\pi 1 \rightarrow \pi 2^*$ configuration. It appears at 3.7 eV and has a calculated oscillator strength of 0.093. The computed vertical excitation is in agreement with the position of the absorption maximum in ethanol[14] and water (∼3.8 eV)[12,15] and the red-shift of that band in DNQSH with respect to DNQ. Finally, the experimental band centered around 4.6−4.7 eV can be assigned to the computed $4^1A'$ and $5^1A'$ states of DNQ and DNQSH, respectively. A similar assignment of the low-energy region of the spectra can be done on the basis of the TD-DFT results (Table SI2). These calculations give a similar character for the three lowest $\pi\pi^*$ excitations in the three compounds of interest, although some of the excitations are shifted by up to 0.5 eV.

The contribution of the $n\pi^*_{NN}$ transition to the spectrum can be not determined precisely because of a suspected inaccuracy of the multistate treatment. Thus, the MS-CASPT2 method is reliable when the multistate correction of the CASPT2 results is small.[29] In the present case, the correction is 0.3 eV or less for all states with the exception of the $n\pi^*_{NN}$ state (Table SI1 in the Supporting Information), whose MS-CASPT2 energies deviate by 0.8−1.1 eV in vacuum and 0.5−0.7 eV in water from the CASPT2 ones. The reason for this large difference is the coupling of the $n\pi^*_{NN}$ state with the lowest lying $\pi\pi^*$ transition, which has the same symmetry and similar CASPT2 energy. The multistate treatment reduces the coupling, but the large value of the correction implies that the MS-CASPT2 energy of the $n\pi^*_{NN}$ state might be overestimated. Therefore, one possible interpretation (based on MS-CASPT2 values) is that this state is hidden below the intense $\pi\pi^*$ transition around 270 nm. Another interpretation (based on CASPT2 excitation energies) is that it is contributing to the structure of the band around ∼300 nm in DNQ and DNQSH. The TD-DFT calculations also predict a substantial degree of mixing between the lowest $\pi\pi^*$ configuration and the $n\pi^*_{NN}$ one, with the $n\pi^*_{NN}$ state appearing at 290 and 287 nm in DNQ and DNQS, respectively.

The absorption profile of the low-energy band in the spectrum of DNQ in ethanol glass[14] shows three different peaks separated by a value of 1300−1500 $cm^{-1}$. The $\pi 1 \rightarrow \pi 1^*$ transition is the only absorbing state around 400 nm, and the peaks must correspond to a vibrational structure. In order to get insight into the origin of this structure, we have calculated the $\gamma_i$ parameter, which is proportional to the Franck−Condon intensity. This parameter is calculated for the totally symmetric modes of the $\pi 1 \rightarrow \pi 1^*$ excited-state minimum of $C_s$ symmetry (Figure 2). The most active vibrations are the 421 $cm^{-1}$ and 1662 $cm^{-1}$ modes, which involve diazo group bending and bond inversion dominated by $C_2-C_3/C_4-C_{10}$ in phase stretching, respectively (Figure 3). The unscaled mode of 1662 $cm^{-1}$ is in reasonable

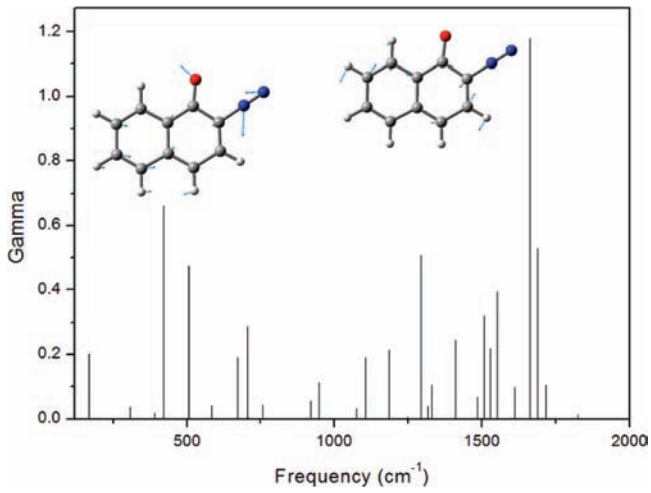


**Figure 3.** Predicted intensities and vectorial representation of the most active vibrational modes in the DNQ $\pi 1 \rightarrow \pi 1^*$ transition.

agreement with the observed separation between the peaks, although other modes will also contribute to the vibrational structure.

The $\pi 1 \rightarrow \pi 1^*$ minimum of $C_s$ symmetry is stabilized by 0.03 eV in vacuum and 0.04 eV in water (MS-CASPT2 level, Table SI3 in the Supporting Information) relative to the FC $\pi 1 \rightarrow \pi 1^*$ energy. This small stabilization indicates that the vertical excitation energy may be underestimated by the multistate treatment (the stabilization at the CASPT2 level is 0.28 eV). Compared to the $S_0$ minimum, the double $C_3-C_4$, $C_9-C_{10}$, $C_2-N_{12}$ bonds are expanded and single $C_4-C_{10}$, $C_2-C_3$ bonds are contracted. A frequency calculation shows that the $C_s$ minimum corresponds to a transition state. The eigenvector associated with the imaginary frequency (290i $cm^{-1}$) corresponds to an out-of-plane mode characterized by $C_2-N_{12}-N_{13}$ out-of-plane bending (Figure 2). Distortion of the $C_s$ minimum along this vector leads to a nonplanar $\pi 1 \rightarrow \pi 1^*$ minimum (Figure 2) located ~1 eV below the $C_s$ minimum, with the diazo group bent and twisted out of the naphthoquinone ring and the $C_2-N_{12}$ bond stretched to 1.45 Å. Comparison of the singly occupied molecular orbitals at the nonplanar minimum (Figure 2) with the corresponding ones of the FC geometry in Figure 1 confirms that this structure correlates diabatically with the $\pi 1 \rightarrow \pi 1^*$ state at the FC geometry.

## Conclusions

The vertical excitations energies of DBQ, DNQ and DNQSH have been calculated at the MS-CASPT2 level in vacuum and in water. This has allowed us to assign the bands excited in the photochemical experiments around 400 and 300 nm. The band around 400 nm corresponds to the lowest $\pi\pi^*$ state and shows a vibrational structure arising from a bond-inversion mode and a bending mode of the diazo group, while the band around 300 nm is assigned to another $\pi\pi^*$ state for DNQ and DNQSH. The calculations also suggest that a nonplanar intermediate that correlates with the lowest $\pi\pi^*$ state may be involved in the photochemical WR induced by excitation at 400 nm. The elongated $C_2-N_{12}$ bond and the out-of-plane bending of the diazo group suggest that the intermediate is prone to C−N bond cleavage. Therefore, while recent experiments point to an ultrafast, concerted reaction,[9] the process may be asynchronous, and the initial phase dominated by nitrogen elimination. In addition to that, the close-lying $\pi\pi^*_{NN}$ state might also be accessed through a conical intersection with the bright state and could also be important for the reactivity. Calculations to clarify the mechanism of the photoinduced WR are currently under way.

**Acknowledgment.** This work has been supported by Project No. CTQ2008-06696 of the Spanish Ministerio de Ciencia e Innovación (MICINN). Q.L. acknowledges a postdoctoral fellowship of MICINN (Programa de ayudas para la contratación de jovenes doctores extranjeros en universidades y centros de investigación españoles, ref SB-2006-0063), and A.M. a postdoctoral fellowship of the Departament d'Innovació, Universitats i Empresa, Generalitat de Catalunya (Beca postdoctoral Beatriu de Pinós, ref 2007 BP-B1 00015).

**Supporting Information Available:** Complete refs 20 and 21. CASSCF, CASPT2, MS-CASPT2 (Table SI1), and TD-B3LYP (Table SI2) vertical excitation energies and oscillator strengths, relative MS-CASPT2 energies of $S_0$ and $\pi 1 \rightarrow \pi 1^*$ states (Table SI3), orbitals of DNQSH at the MS-CASPT2 level (Figure SI1) and TD-B3LYP orbitals (Figure SI2), and Cartesian coordinates for all minimum structures. This material is available free of charge via the Internet at http://pubs.acs.org.

## References and Notes

(1) Wolff, L. *Justus Liebigs Ann. Chem.* **1902**, *325*, 129–133.
(2) Livinghouse, T.; Stevens, R. V. *J. Am. Chem. Soc.* **1978**, *100*, 6479–6482.
(3) Stevens, R. V.; Bisacchi, G. S.; Goldsmith, L.; Strouse, C. E. *J. Org. Chem.* **1980**, *45*, 2708–2709.
(4) Cheng, J.; Ziller, J. W.; Deming, T. J. *Org. Lett.* **2000**, *2*, 1943–1946.
(5) Nakatani, K.; Shirai, J.; Tamaki, R.; Saito, I. *Tetrahedron Lett.* **1995**, *36*, 5363–5366.
(6) Nakatani, K.; Shirai, J.; Sando, S.; Saito, I. *J. Am. Chem. Soc.* **1997**, *119*, 7626–7635.
(7) Martin, P.; Winkler, T. *Helv. Chim. Acta* **1993**, *76*, 1674–1677.
(8) Kirmse, W. *Eur. J. Org. Chem.* **2002**, 2193–2256.
(9) Wolpert, D.; Schade, M.; Brixner, T. *J. Chem. Phys.* **2008**, *129*, 094504.
(10) Burdzinski, G. T.; Wang, J.; Gustafson, T. L.; Platz, M. S. *J. Am. Chem. Soc.* **2008**, *130*, 3746–3747.
(11) Reiser, A.; Huang, J. P.; He, X.; Yeh, T. F.; Jha, S.; Shih, J. Y.; Kim, M. S.; Han, Y. K.; Yan, K. *Eur. Polym. J.* **2002**, *125*, 619–629.
(12) Tanigaki, K.; Ebbesen, T. W. *J. Phys. Chem.* **1989**, *93*, 4531–4536.
(13) Schweig, A.; Baumgartl, H.; Schulz, R. *J. Mol. Struct.* **1991**, *247*, 135–171.
(14) Vleggaar, J. J. M.; Huizer, A. H.; Kraakman, P. A.; Nijssen, W. P. M.; Visser, R. J.; Varma, C. A. G. O. *J. Am. Chem. Soc.* **1994**, *116*, 11754–11763.
(15) Tanigaki, K.; Ebbesen, T. W. *J. Am. Chem. Soc.* **1987**, *109*, 5883–5884.
(16) Barra, M.; Fisher, T. A.; Cernigliaro, G. J.; Sinta, R.; Scaiano, J. C. *J. Am. Chem. Soc.* **1992**, *114*, 2630–2634.
(17) Ershov, V. V.; Nikiforov, G. A.; De Jonge, C. R. H. I. In *Quinone Diazides*; Davidson, T., Ed.; Elsevier: Amsterdam, Oxford, New York, 1981.
(18) Miller, R. D.; McKean, D. R.; Tompkins, T. L.; Willson, C. G.; Michl, J.; Downing, J. In *Polymers in Electronics*; Davidson, T., Ed.; ACS Symposium Series 242; American Chemical Society: Washington, DC, 1984.
(19) Ghigo, G.; Roos, B. O.; Malmqvist, P. A. *Chem. Phys. Lett.* **2004**, *396*, 142–149.
(20) Karlstrom, G.; Lindh, R.; Malmqvist, P. A.; et al. *Comput. Mater. Sci.* **2003**, *28*, 222–239.
(21) Frisch, M. J.; Trucks, G. W.; Schlegel, H. B.; *Gaussian 03, Version B.02*; Gaussian, Inc.: Pittsburgh, PA, 2003.
(22) Leyva, V.; Corral, I.; Schmierer, T.; Heinz, B.; Feixas, F.; Migani, A.; Blancafort, L.; Gilch, P.; González, L. *J. Phys. Chem. A* **2008**, *112*, 5046–5053.
(23) Negri, F.; Zgierski, M. Z. *J. Chem. Phys.* **1993**, *99*, 4318–4326.
(24) Malmqvist, P. A.; Roos, B. O.; Schimmelpfennig, B. *Chem. Phys. Lett.* **2002**, *357*, 230–240.
(25) Barone, V.; Cossi, M. *J. Phys. Chem. A* **1998**, *102*, 1995–2001.
(26) Cossi, M.; Rega, N.; Scalmani, G.; Barone, V. *J. Chem. Phys.* **2001**, *114*, 5691–5710.
(27) Cossi, M.; Barone, V. *J. Chem. Phys.* **2000**, *112*, 2427–2435.
(28) Platt, J. R. *J. Chem. Phys.* **1949**, *17*, 484–495.
(29) Serrano-Andrés, L.; Merchán, M.; Lindh, R. *J. Chem. Phys.* **2005**, *122*, 104107.

JP904853C